Available online at www.sciencedirect.com

SCIENCE DIRECT

Journal of Solid State Chemistry 179 (2006) 1016–1021

JOURNAL OF SOLID STATE CHEMISTRY

www.elsevier.com/locate/jssc

Synthesis and crystal structures of La_3MgBi_5 and $LaLiBi_2$

Da-Chun Pan, Zhong-Ming Sun, Jiang-Gao Mao*

State Key Laboratory of Structural Chemistry, Fujian Institute of Research on the Structure of Matter, Chinese Academy of Sciences, Fuzhou 350002, People's Republic of China

Received 3 October 2005; received in revised form 11 December 2005; accepted 17 December 2005
Available online 20 January 2006

Abstract

Two new ternary bismuthides, La_3MgBi_5 and $LaLiBi_2$, have been prepared by solid-state reactions of the corresponding pure metals in welded niobium tubes at high temperature. Their structures have been established by single-crystal X-ray diffraction studies. La_3MgBi_5 crystallizes in the hexagonal space group $P6_3/mcm$ (No.193) with cell parameters of $a = b = 9.7882(7)$ Å, $c = 6.5492(9)$ Å, $V = 543.41(9)$ Å^3, and $Z = 2$. $LaLiBi_2$ belongs to tetragonal space group $P4/nmm$ (No.129) with cell parameters of $a = b = 4.5206(4)$ Å, $c = 10.9942(19)$ Å, $V = 224.68(5)$ Å^3, and $Z = 2$. The structure of La_3MgBi_5 is of the "anti" Hf_5Sn_3Cu type, and features 1D linear Bi^- anionic chains and face-sharing $[MgBi_{6/2}]^{7-}$ octahedral chains. The structure of $LaLiBi_2$ is isotypic with $HfCuSi_2$, and is composed of 2D Bi^- square sheets and 2D LiBi layers with La^{3+} ions as spacers. Band calculations indicate that both compounds are metallic.

Keywords: Polar intermetallics; Solid-state reaction; Crystal structure; Bismuth compound; Mixed cation method

1. Introduction

During the past three decades, considerable efforts have been devoted to the studies of the ternary rare-earth transition metal antimonides, $RE_xM_ySb_z$ [1–18]. These antimonides exhibit varied electrical and magnetic properties arising from the interaction of *f* and *d* electrons. Most of compounds have been structurally determined by single crystal X-ray diffraction. Several examples include RE_3MSb_5 ($M =$ Ti, Zr, Hf, Nb) with the hexagonal Hf_5Sn_3Cu structure [1–4], whose structure features chains of face-sharing MSb_6 octahedra and linear Sb chains; $REMSb_2$ ($M =$ Mn–Zn, Pd, Ag, Au) with the $HfCuSi_2$ structure [5–13], which is composed of 2D Sb^- square sheet and $[MSb]^{2-}$ layers with lanthanide cations as spacers, and $REMSb_3$ ($M =$ Cr, V) [14–18]. It is interesting to note that $LaCrSb_3$ exhibits ferromagnetic ordering at $T_C = 120-140$ K and a spin-reorientation transition at $T_{sr} = 95$ K [18]. The corresponding transition metal bismuth analogs are relatively rare. A few Bi phases reported are $RE_{14}MPn_{11}$ ($RE =$ Eu, Yb; $M =$ Mn, In; $Pn =$ Sb, Bi) with a $Ca_{14}AlSb_{11}$ structure [19,20], RE_5M_2Pn ($M =$ Ni, Pd; $Pn =$ Sb, Bi) with a Mo_5B_2Si structure [21]; $REMPn$ ($M =$ Rh, Ni; $Pn =$ Sb, Bi) with a TiNiSi structure [22], and $Yb_9Zn_4Bi_9$ features $[Zn_4Bi_9]^{19-}$ ribbons running along the *c*-axis [23].

It is possible that Li and Mg metals may replace the transition metals in above phases to form new polar intermetallic phases. Moreover, using two types of cations with different size and charge has been found to be an effective route for the preparation of novel polar intermetallic phases, due to the lessening of cation packing limitation and changing of electronic requirements [24–28]. The aim of our study is to explore the new intermetallic *Ln*–Li(Mg)–Bi ternary phases and to understand their crystal structures and chemical bonding as well as their electronic properties. By using this synthetic strategy, we have successfully synthesized two new rare-earth bismuth ternary phases, namely, La_3MgBi_5 and $LaLiBi_2$. Herein, we report their syntheses, crystal structures, and chemical bonding.

*Corresponding author. Fax: +86 591 371 4946.
E-mail address: mjg@ms.fjirsm.ac.cn (J.-G. Mao).

0022-4596/$ - see front matter © 2006 Elsevier Inc. All rights reserved.
doi:10.1016/j.jssc.2005.12.030

2. Experimental

2.1. Synthesis

All manipulations were performed inside an argon-filled glove box with moisture level below 1 ppm. Magnesium turnings (99.9%, Acros), lithium ingot (99.9%, Aldrich), lanthanum chip (99.9%, Aldrich) and bismuth block (99.9%, Alfa) were used as received. Single crystals of La_3MgBi_5 were initially obtained by the solid-state reaction of magnesium (0.012 g, 0.5 mmol), lanthanum (0.138 g, 1.0 mmol) and bismuth (0.313 g, 1.5 mmol). The mixture was loaded into a niobium tube, arc-welded and then sealed in an evacuated quartz tube ($\sim 10^{-4}$ Torr). The tube was put into an oven and heated at 980 °C for 2 days, and annealed at 800 °C for 7 days. Afterwards, the reaction tube was allowed to cool at a rate of 0.1 °C/min to the room temperature. Brick-shaped gray crystals of La_3MgBi_5 were obtained. Single crystals of $LaLiBi_2$ (brick in shape and gray in color) were obtained in a similar way by using lithium (0.069 g, 1.0 mmol) instead of magnesium. Several single crystals of La_3MgBi_5 and $LaLiBi_2$ were analyzed by using energy-dispersive X-ray spectroscopy (EDAX 9100), and the results indicate that atomic ratios to be 2.8: 1.0: 5.1 for La, Mg, and Bi in La_3MgBi_5 and 1: 2.2 for La and Bi in $LaLiBi_2$, respectively, which are in good agreement with those of the structural refinements. After the determination of single crystal structures, great efforts were subsequently made to synthesize pure phases of La_3MgBi_5 and $LaLiBi_2$. The reactions were carried out in a stoichiometric ratio of the metals, as well as using of an excess of ~20% lithium to compensate possible loss during arc welding. The samples were heated at 980 °C for 1 day, quenched in water, and annealing at different temperatures (600, 700, 800, and 850 °C, respectively, for each individual reaction) for 1 month. However, X-ray powder patterns of the resultant products revealed the presence of impurity phases, such as LaBi (*Fm3-m*), Mg_3Bi_2 (*P3-m1*), as well as other unidentified compounds. Attempts were also made to obtain the $LaMgBi_2$ phase, but only La_3MgBi_5 was formed. The highest yields of ~60% and ~70%, for La_3MgBi_5 and $LaLiBi_2$, were obtained by annealing at 800 and 700 °C, respectively. Physical properties were not measured due to the difficulty to obtain mono-phase products.

2.2. Crystal structure determination

Single crystals of La_3MgBi_5 (size: $0.15 \times 0.07 \times 0.04\,mm^3$) and $LaLiBi_2$ (size: $0.12 \times 0.12 \times 0.10\,mm^3$) were selected from the reaction products and sealed within thin-walled glass capillaries under an argon atmosphere. Data collections for both compounds were performed on a Rigaku Mercury CCD (Mo$K\alpha$ radiation, graphite monochromator) at room temperature. A total of 255 and 191 independent reflections for La_3MgBi_5 and $LaLiBi_2$, respectively, were measured, of which 238 and 176 reflections with $I > 2\sigma(I)$ were considered observed. Both data sets were corrected for Lorentz factor, polarization, air absorption and absorption due to variations in the path length through the detector faceplate. Absorption corrections based on Multi-scan method were also applied [29].

Both structures were solved using direct methods (SHELXTL) and refined by least-square methods with atomic coordinates and anisotropic thermal parameters [30]. The final stage of least-squares refinement showed no abnormal behaviors in the occupancy factors. The larger thermal parameters and their standard deviations in $LaLiBi_2$ are due to that the lithium atom is very light. Final difference Fourier maps showed featureless residual peaks of 3.208 (0.87 Å from Bi(1)) and $-2.477\,e\text{Å}^{-3}$ (0.65 Å from Bi(2)) for La_3MgBi_5; 4.688 (1.20 Å from La(1)) and $-2.670\,e\text{Å}^{-3}$ (1.18 Å from Bi(2)) for $LaLiBi_2$, respectively. The relatively higher residual peaks were due to the fact that bismuth element in the compound has a large atomic number, which may result in absorption correction problem and higher residual peaks. Crystal data and further details of data collection are given in Table 1, and the atomic coordinates, important bond lengths and angles are listed in Tables 2 and 3, respectively. Crystallographic data in CIF format for La_3MgBi_5 and $LaLiBi_2$ have been deposited as CSD number 415727 and 415728. These data may be obtained free of charge by contacting FIZ Karlsruhe at +49 7247 808 666 (fax) or crysdata@fizkarlsruhe.de (E-mail).

2.3. Band structure

3D band structure calculations for La_3MgBi_5 and $LaLiBi_2$ along with the Density of States (DOS) and Crystal Orbital Overlap Population (COOP) curves were performed using the Crystal and Electronic Structure Analyzer (CAESAR) software package [31]. The following atomic orbital energies and exponents were employed for the calculations (H_{ii} = orbital energy, ζ = Slater exponent): La 6s, $H_{ii} = -6.56$ eV, $\zeta = 2.14$; 6p, $H_{ii} = -4.38$ eV, $\zeta = 2.08$; 5*d*, $H_{ii} = -7.52$ eV, $\zeta = 3.78$ [32]; Bi 6s, $H_{ii} = -15.19$ eV, $\zeta = 2.56$; 6p, $H_{ii} = -7.79$ eV, $\zeta = 2.07$; Mg 3s, $H_{ii} = -9.00$ eV, $\zeta = 1.10$; 3p, $H_{ii} = -4.50$ eV, $\zeta = 1.11$; Li 2s, $H_{ii} = -5.40$ eV, $\zeta = 0.65$; 2p, $H_{ii} = -3.50$ eV, $\zeta = 0.65$.

3. Results and discussion

By using the "mixed cation" method, we obtained two new ternary bismuth phases, La_3MgBi_5 and $LaLiBi_2$. Results also indicate that magnesium and lithium can replace the transition metals in *Ln*–*TM*–Bi systems.

As shown in Fig. 1, La_3MgBi_5 can be regarded as an "anti"-type structure of Hf_5Sn_3Cu with the bismuth atoms on the hafnium sites, and lanthanum and magnesium atoms occupy the tin and copper sites, respectively. It is also isostructural with RE_3MSb_5 (M = Ti, Zr, Hf, Nb) reported previously [1–4]. Bi(2) atoms form a linear chain along the *c*-axis (Fig. 2a). Within the Bi chains, the Bi–Bi distance of 3.2746(5) Å corresponds to a Pauling

Table 1
Summary of crystal data and structure refinement for La_3MgBi_5 and $LaLiBi_2$

Formula	La_3MgBi_5	$LaLiBi_2$
Fw/g mol^{-1}	1485.94	563.81
Space group	$P6_3/mcm$ (no.193)	$P4/nmm$ (no.129)
a/Å	9.7882(7)	4.5206(4)
c/Å	6.5492(9)	10.9942(19)
V, Å^3	543.41(9)	224.68(5)
Z	2	2
D_{calcd}, g cm^{-3}	9.081	8.334
μ, mm^{-1}	92.147	87.239
F(000)	1196	452
Size (mm)	0.15 × 0.07 × 0.04	0.12 × 0.12 × 0.10
Color and habit	Gray, brick	Gray, brick
Hkl range	±12, ±12, $-8<l<5$	$-4<h<5$, ±5, ±14
Reflections collected	3947	1723
Unique reflections	255 (R_{int} = 12.38%)	191 (R_{int} = 7.46%)
Reflections ($I>2\sigma(I)$)	238	176
GOF on F^2	1.133	1.115
R_1, wR_2 ($I>2\sigma(I)$)[a]	0.0355/0.0796	0.0275/0.0666
R_1, wR_2 (all data)	0.0387/0.0811	0.0296/0.0676
Residual extremes (eÅ^{-3})	3.208 (0.87 Å from Bi(1)) and −2.477 (0.65 Å from Bi(2))	4.826 (1.20 Å from La(1)) and −2.667 (1.18 Å from Bi(2))

[a] $R_1=\sum\|F_o|-|F_c\|/\sum|F_o|$, $wR_2=\{\sum w[(F_o)^2-(F_c)^2]^2/\sum w[(F_o)^2]^2\}^{1/2}$.

Table 2
Atomic coordinates and equivalent thermal parameters (× 10^3 Å^2) for La_3MgBi_5 and $LaLiBi_2$

Atom	Wyckoff site	x	y	z	U_{eq}[a]
La_3MgBi_5					
La(1)	6g	0.6193(2)	0	1/4	9 (1)
Mg(1)	2b	0	0	0	9 (3)
Bi(1)	6g	0.2656(1)	0	1/4	9 (1)
Bi(2)	4d	1/3	2/3	0	7 (1)
$LaLiBi_2$					
La(1)	2c	1/4	1/4	0.7383(1)	4 (1)
Li(1)	2a	3/4	1/4	0	38 (19)
Bi(1)	2b	3/4	1/4	0.5	5 (1)
Bi(2)	2c	1/4	1/4	0.1620(1)	5 (1)

[a] U_{eq} is defined as one third of the trace of the orthogonalized U_{ij} tensor.

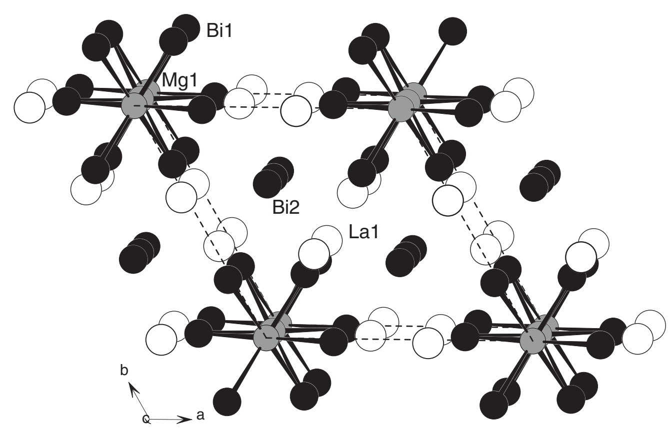

Fig. 1. View of the structure of La_3MgBi_5 down the c-axis. The Mg, La and Bi atoms are drawn as gray, white and black circles, respectively.

Table 3
Important bond lengths (Å) and angles (°) for La_3MgBi_5 and $LaLiBi_2$

La_3MgBi_5			
Mg(1)–Bi(1)	3.0725(8) × 6	Bi(2)–Bi(2)	3.2746(5) × 2
La(1)–Bi(1)	3.310(1) × 2	La(1)–Bi(1)	3.4629(7) × 2
La(1)–Bi(1)	3.462(2)	La(1)–Bi(2)	3.4683(6) × 4
Bi(2)–Bi(2)–Bi(2)	180.0	Bi(1)–Mg(1)–Bi(1)	85.75(1) × 6
Bi(1)–Mg(1)–Bi(1)	94.24(1) × 6	Bi(1)–Mg(1)–Bi(1)	180.00(2) × 3
$LaLiBi_2$			
Li(1)–Bi(2)	2.8775(7) × 4	Bi(1)–Bi(1)	3.1965(3) × 4
La(1)–Bi(1)	3.460(1) × 4	La(1)–Bi(2)	3.3793(6) × 4
Bi(1)–Bi(1)–Bi(1)	180.0 × 2	Bi(1)–Bi(1)–Bi(1)	90.0 × 4
Bi(2)–Li(1)–Bi(2)	112.52(2) × 4	Bi(2)–Li(1)–Bi(2)	103.53(3) × 2

single bond, and is slightly longer than that of the zig-zag Bi chains (3.225 Å) in $EuBi_2$ [33], but very close to the Bi–Bi bond of the dumbbell (3.27 Å) in $Sr_{11}Bi_{10}$ [34]. It should be pointed out that the corresponding Sb–Sb bond lengths of ~3.10 Å in those RE_3MSb_5 systems are too longer to be viewed as a Sb–Sb single bond (2.908 Å) [1–3]. The Mg atoms are six-coordinated by six Bi(1) atoms in an octahedral geometry (Fig. 2b). The Mg–Bi distances are 3.0725(8) Å. These $MgBi_6$ octahedra form an infinite chain along the c-axis via face-sharing (Fig. 2b). The La atom in La_3MgBi_5 is nine-coordinated by five Bi(1) and four Bi(2) atoms with La–Bi distances of 3.310(1)–3.4683(6) Å (Table 3), which are comparable to the sum of covalent radii of La and Bi atoms (3.47 Å). Its

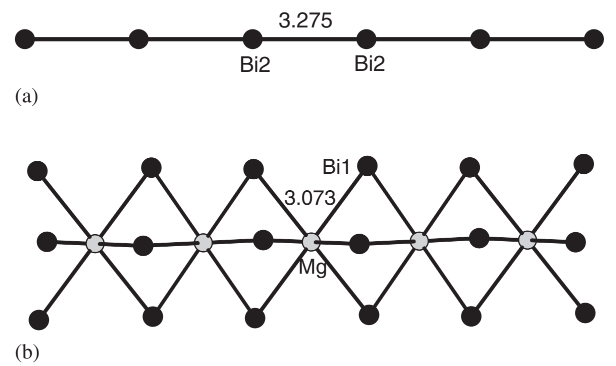

Fig. 2. The drawing of a 1D liner chain of Bi^- (a) and a face-sharing $[MgBi_{6/2}]^{7-}$ octahedral chain (b) in La_3MgBi_5.

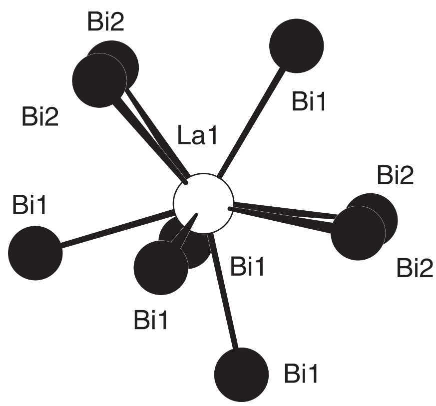

Fig. 3. The coordination geometry around the lanthanum atom in La_3MgBi_5.

coordination geometry can be described as a distorted tricapped trigonal prism (Fig. 3).

$LaLiBi_2$ belongs to the $HfCuSi_2$ structure type. As shown in Fig. 4, its structure features 2D Bi^- square sheets and corrugated $LiBi^{2-}$ layer with La^{3+} ions as spacers. The 2D Bi^- square sheet shown in Fig. 5a is similar to that in $EuBi_2$ [33]. However, the Bi–Bi distance of 3.1965(3) Å is slightly longer than that of element bismuth (3.072 Å) [35], but is significantly shorter than that of the bismuth square net in $EuBi_2$ (3.3442 Å). Each lithium atom is surrounded by four Bi(2) neighbors in a tetrahedral geometry and each Bi(2) atom is also tetrahedrally coordinated by four Li atoms. The Li–Bi distance is 2.8776(7) Å (Table 3). These $LiBi_4$ tetrahedra are further interconnected via edge- and corner-sharing into a ⟨001⟩ corrugated LiBi layer (Fig. 5b). The Bi–Li–Bi angles are 112.52(2)° and 103.53(3)°, respectively (Table 3). The La^{3+} ion is eight-coordinated by four Bi(1) and four Bi(2) atoms in a distorted square anti-prismatic geometry (Fig. 6). The La–Bi distances are in the range of 3.3794(6)–3.460(1) Å (Table 3).

The electron count scheme for both La_3MgBi_5 and $LaLiBi_2$ can be developed by using the "hypervalent" bond electron counting method as well as Zintl–Klemn concept [24,36]. It is interesting to examine the chemical bonding of

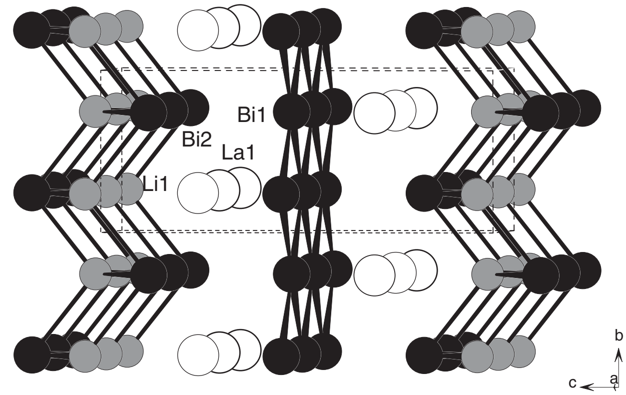

Fig. 4. View of the structure of $LaLiBi_2$ down the *a*-axis. The Li, La and Bi atoms are drawn as gray, white and black circles, respectively.

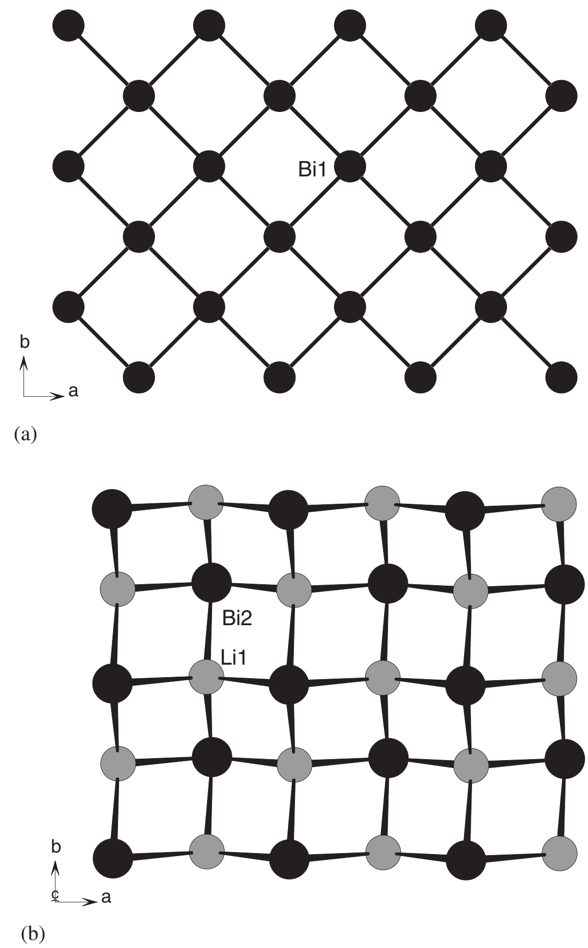

Fig. 5. A 2D square sheet of Bi^- (a) and a ⟨001⟩ corrugated LiBi layer (b) in $LaLiBi_2$.

the linear Bi chains in La_3MgBi_5, which is different from that of the linear Sb chain in La_3MSb_5 (M = Zr, Hf) [2]. The Sb–Sb distance of about ~3.20 Å for the linear Sb chain in La_3MSb_5 (M = Zr, Hf) is a typical "hypervalent bond" and each Sb can be assigned to be −2 in charge [2]. The present Bi linear chain has a Bi–Bi distance of

3.2746(5) Å, which is comparable to that of zig-zag Bi chain in $EuBi_2$ [33]. Hence it is more reasonable to assign −1 charge rather than −2 for each Bi. The lower charge associated with the Bi chain in La_3MgBi_5 is also due to lower positive charge for Mg^{2+} compared with Zr^{4+} or Hf^{4+} in La_3MSb_5 (M = Zr, Hf) [2]. Such assignment is also supported by the results from band structure calculations, which will be discussed later. Therefore, La_3MgBi_5 can be formulated as $[(La^{3+})_3(Mg^{2+})(_{chain}Bi^{1-})_2(_{isolated}Bi^{3-})_3]$. The Sb chain in U_3MnSb_5 is also assigned to be −1 per Sb whereas two negative charges per Sb is assigned to the linear Sb chain in U_3TiSb_5 [4]. For $LaLiBi_2$, similar to that in the Sb^- square net, each Bi(1) atom of the 2D square sheet in $LaLiBi_2$ is −1 according to the concept of "hypervalent" bonding [24]. Bi(2) atom of the $LiBi^{2-}$ layer is not involved in Bi–Bi bonding interaction, it is considered to be "isolated" and assigned to be −3 according to Zintl–Klemn concept [36]. Hence $LaLiBi_2$ can be formulated as $(La^{3+})(Li^+)[(_{square}Bi^{1-})(_{isolated}Bi^{3-})]$. The above formulations are sometimes invalid due to the incompleteness of electron transfer from cations to the anionic network. Lanthanide metals such as La usually participate in significant bonding interaction with the anionic network, so do Li and Mg metals.

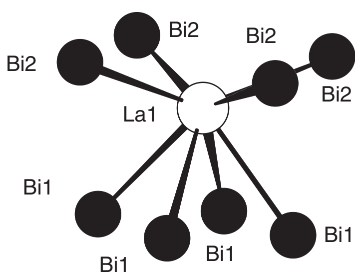

Fig. 6. Coordination geometry around the lanthanum atom in $LaLiBi_2$.

To further understand the chemical bonding of La_3MgBi_5 and $LaLiBi_2$, 3D band structure calculations have been performed by using CAESAR program [31]. Results are shown in Figs. 7 and 8. There are no observable band gaps around the Fermi level for both compounds, indicating that both compounds are metallic. The states just below and above Fermi level are predominately from p-orbitals of the bismuth and d-orbitals of the lanthanum atoms. The states below −14 eV are predominately from s-orbitals of the bismuth atoms. The contributions from lithium or magnesium atoms to the DOS states around the Fermi level are very small. The COOP curves are more informative. For La_3MgBi_5, the average OP values for Bi–Bi (3.275 Å), La–Bi (3.3–3.5 Å) and Mg–Bi (3.072 Å) are 0.278, 0.295 and 0.249, respectively, which indicate

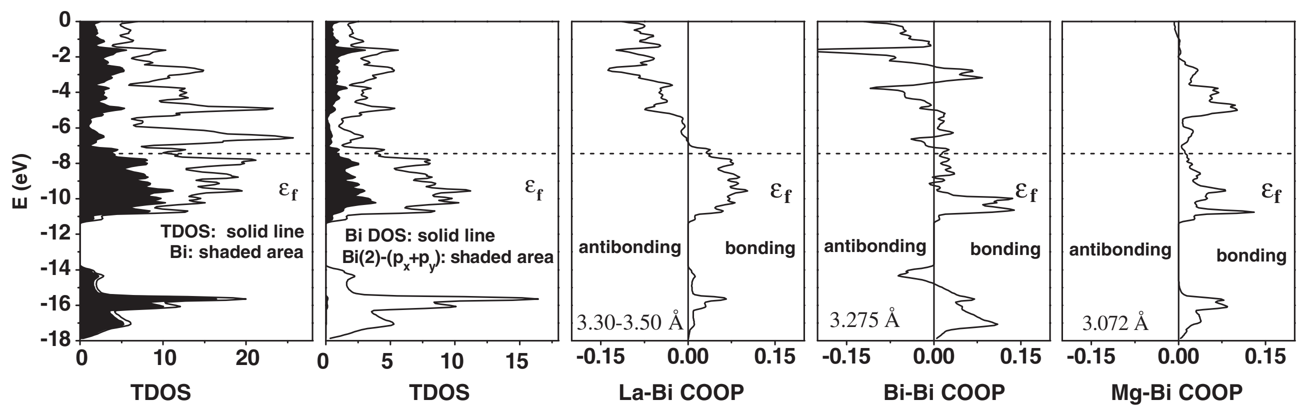

Fig. 7. Density of State (with the Bi projection shown by the filled area), La–Bi, Bi–Bi and Mg–Bi coop curves for La_3MgBi_5. The Fermi level is set to −7.44 eV.

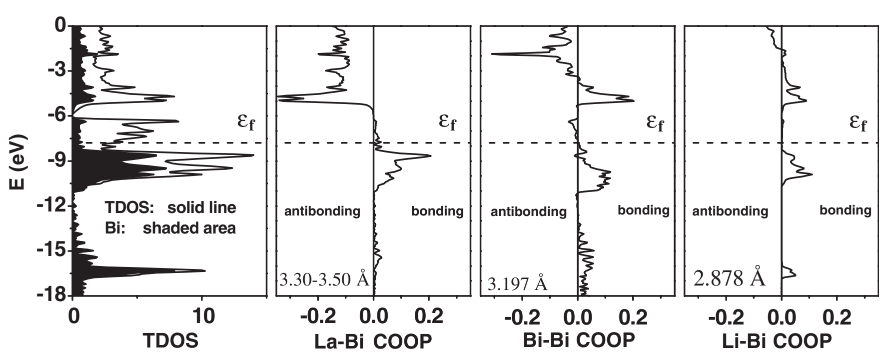

Fig. 8. Density of State (with the Bi projection shown by the filled area), La–Bi, Bi–Bi and Li–Bi coop curves for $LaLiBi_2$. The Fermi level is set to −7.79 eV.

significant Bi–Bi, La–Bi, Mg–Bi bonding interactions. The Bi–Bi interaction is weakly bonding around the Fermi level. Such interaction is composed of significant σ_{Bi-Bi} interaction as well as weak π_{Bi-Bi} interaction, since states around the Fermi level show significant contributions from the Bi(2) p_x and p_y orbitals in addition to p_z characters. The weak $\pi \ldots \pi$ bonding interaction may be responsible to the shorter Bi–Bi distance in La_3MgBi_5 compared to that in a normal "hypervalent" Bi linear chain. For $LaLiBi_2$, the Bi–Bi bond (3.197 Å) has a larger average OP value of 0.337, and the La–Bi (3.3–3.5 Å) and Li–Bi (2.878 Å) are also significantly bonding with average OP values of 0.262 and 0.129, respectively. The strong La–Bi, Mg–Bi and Li–Bi interactions in both compounds are responsible for their metallic behavior.

4. Conclusion remarks

In conclusion, two new ternary bismuthides, La_3MgBi_5 and $LaLiBi_2$, have been prepared and structurally elucidated. Both La_3MgBi_5 and $LaLiBi_2$ contain an alkaline earth or alkali metal, Li^+ and Mg^{2+} are similar in many aspects, hence the structures of La_3MgBi_5 and $LaLiBi_2$ have many similar features. Firstly, "hypervalent" bonding units are present in both phases, 1D chain in La_3MgBi_5 and 2D square sheet in $LaLiBi_2$. Secondly, some Bi atoms involve in non-Bi–Bi bonding interactions and only connected with Li^+ or Mg^{2+} cations, face-sharing $[MgBi_{6/2}]^{7-}$ octahedral chains in La_3MgBi_5 and 2D corrugated $LiBi^{2-}$ layers in $LaLiBi_2$. Hence the two phases are closely related.

Acknowledgments

This work was supported by the National Natural Science Foundation of China (Grant no. 20573113) and NSF of Fujian province (no. E0320003). We thank for the helpful suggestion from Prof. Li-Ming Wu.

References

[1] G. Bolloré, M.J. Ferguson, R.W. Hushagen, A. Mar, Chem. Mater. 7 (1995) 2229.
[2] M.J. Ferguson, R.W. Hushagen, A. Mar, J. Alloys Compd. 249 (1997) 191.
[3] S.H.D. Moore, L. Deakin, M.J. Ferguson, A. Mar, Chem. Mater. 14 (2002) 4867.
[4] M. Brylak, W. Jeitschko, Z. Naturforsch. B 49 (1994) 747.
[5] G. Cordier, H. Schäfer, P. Woll, Z. Naturforsch. B 40 (1985) 1097.
[6] D. Kaczorowski, J. Alloys Compd. 186 (1992) 333.
[7] A. Leithe-Jasper, P. Rogl, J. Alloys Compd. 203 (1994) 133.
[8] M. Brylak, M.H. Möller, W. Jeitschko, J. Solid State Chem. 115 (1995) 305.
[9] P. Wollesen, W. Jeitschko, M. Brylak, L. Dietrich, J. Alloys Compd. 245 (1995) L5.
[10] L. Gondek, B. Penc, A. Szytula, N. Stusser, J. Alloys Compd. 346 (2002) 80.
[11] Z. Bukowski, V.H. Tran, J. Stepień-Damm, R. Troć, J. Solid State Chem. 177 (2004) 3934.
[12] A. Szytuła, A. Kolenda, A. Oleś, J. Alloys Compd. 383 (2004) 224.
[13] M. Brylak, W.Z. Jeitschko, Naturforsch. B: Chem. Sci. 49 (1994) 747.
[14] M. Brylak, W. Jeitschko, Z. Naturforsch. B: Chem. Sci. 50 (1995) 899.
[15] S.J. Crerar, L. Deakin, A. Mar, Chem. Mater. 17 (2005) 2780.
[16] E.L. Thomas, R.T. Macaluso, H.O. Lee, Z. Fisk, J.Y. Chan, J. Solid State Chem. 177 (2004) 4228.
[17] R.T. Macaluso, D.M. Wells, R.E. Sykora, T.E. Albrecht-Schmitt, A. Mar, S. Nakatsuji, H. Lee, Z. Fisk, J.Y. Chan, J. Solid State Chem. 177 (2004) 293.
[18] N.P. Raju, J.E. Greedan, M.J. Ferguson, A. Mar, Chem. Mater. 10 (1998) 3630.
[19] J.Y. Chan, M.E. Wang, A. Rehr, S.M. Kauzlarich, Chem. Mater. 9 (1997) 2131.
[20] J.Y. Chan, M.E. Wang, S.M. Kauzlarich, Chem. Mater. 10 (1998) 3583.
[21] Y. Mozharivskyj, H.F. Franzen, J. Solid State Chem. 152 (2000) 478.
[22] M.G. Haase, T. Schmidt, C.G. Richter, H. Block, W. Jeitschko, J. Solid State Chem. 168 (2002) 18.
[23] S.-J. Kim, J. Salvador, D. Bilc, S.D. Mahanti, M.G. Kanatzidis, J. Am. Chem. Soc. 123 (2001) 12704.
[24] G.A. Papoian, R. Hoffmann, Angew. Chem. Int. Ed 39 (2000) 2408.
[25] Z.M. Sun, J.G. Mao, D.C. Pan, Inorg. Chem. 44 (2005) 6545.
[26] J.G. Mao, J. Goodey, A.M. Guloy, Inorg. Chem. 43 (2004) 282.
[27] I. Todorov, S.C. Sevov, Inorg. Chem. 44 (2005) 5361.
[28] I. Todorov, S.C. Sevov, Inorg. Chem. 43 (2004) 6490.
[29] CrystalClear version 1. 3. 5. Rigaku Corporation, Woodlands, TX, 1999.
[30] G.M. Sheldrick, SHELXTL, version 5.03, Siemens Analytical X-ray Instruments, Madison, WI, 1995;
G.M. Sheldrick, SHELX-96 Program for Crystal Structure Determination, 1996.
[31] J. Ren, W. Liang, M.-H. Whangbo, CAESAR for windows; Prime-Color Software, Inc., North Carolina State University, Raleigh, NC, 1998.
[32] M.J. Ferguson, R.E. Ellenwood, A. Mar, Inorg. Chem. 38 (1999) 4503.
[33] Z.M. Sun, J.G. Mao, J. Solid State Chem. 177 (2004) 3752.
[34] G. Derrien, M. Tillard-Charbonnel, A. Manteghetti, L. Monconduit, C. Belin, J. Solid State Chem. 164 (2002) 169.
[35] J. Donohue, The Structures of the Elements, Wiley, New York, 1974.
[36] G. Miller, in: S. Kauzlarich (Ed.), Chemistry, Structure and Bonding of Zintl Phases and Ions, VCH Publisher, New York, 1996 p61;
J.D. Corbett, in: S. Kauzlarich (Ed.), Chemistry, Structure and Bonding of Zintl Phases, VCH Publisher, New York, 1996 p139.